J|A|C|S
COMMUNICATIONS

Published on Web 12/04/2008

Visible Light Responsive Pristine Metal Oxide Photocatalyst: Enhancement of Activity by Crystallization under Hydrothermal Treatment

Fumiaki Amano,[†,‡] Akira Yamakata,[†,‡] Kohei Nogami,[‡] Masatoshi Osawa,[†,‡] and Bunsho Ohtani*[,†,‡]

Catalysis Research Center, Hokkaido University, Sapporo 001-0021, Japan, and Graduate School of Environmental Science, Hokkaido University, Sapporo 060-0810, Japan

Received September 19, 2008; E-mail: ohtani@cat.hokudai.ac.jp

Photocatalysts for purification of indoor air should induce complete oxidative decomposition of organic pollutants into carbon dioxide (CO_2), i.e., mineralization, preferably under irradiation of visible light (vis) emitted from lighting devices such as fluorescent light tubes. Recently, development of vis-responsive photocatalysts has been accelerated due to findings of activity of surface-modified tungsten(VI) oxide (WO_3) particles for molecular oxygen reduction.[1] Abe et al. reported that platinum-loaded WO_3 particles exhibited vis-induced photocatalytic activity as high as that of titanium(IV) oxide (TiO_2) particles under ultraviolet-light (UV) irradiation.[1a]

The activity of semiconductor photocatalysts depends on physical and chemical properties. Since recombination of photoexcited electrons and holes seems to occur at crystal lattice defects, crystallinity (i.e., the extent of crystallization) should be one of the main factors for photocatalytic reaction efficiency.[2] However, there have been few studies indicating a correlation between crystallinity, recombination rate, and photocatalytic activity. It is difficult to evaluate the effect of only one property on photocatalytic activity excluding effects of other properties.[3] For example, crystallization of amorphous metal oxides by heat treatment resulted in simultaneous changes in other properties such as specific surface area, which is another main factor for reaction efficiency.

In this study, two bismuth tungstate (Bi_2WO_6) samples of almost the same specific surface areas containing only the amorphous or crystalline phase were prepared by hydrothermal reaction of a precursor under the same synthesis conditions except for temperature. Here, for the first time, negligible photocatalytic activity of amorphous Bi_2WO_6 owing to the fast recombination of electron−hole pairs and, in contrast, relatively high quantum efficiency of Bi_2WO_6 crystallites for complete oxidative decomposition of gaseous acetaldehyde (AcH) even under vis irradiation owing to the slow recombination were unambiguously demonstrated by action spectrum analysis and time-resolved infrared (IR) absorption measurements.

Precipitates from reaction between bismuth nitrate and an aqueous solution of sodium tungstate were autoclaved at 373 or 403 K for 20 h, followed by drying at 393 K. X-ray diffraction (XRD) pattern and Raman spectrum analyses of the sample autoclaved at 403 K (BW-cryst) indicate the presence of Bi_2WO_6 crystallites with the mineral name of russellite (Figure 1). Russellite has an orthorhombic structure consisting of layers of WO_6 octahedra sandwiched between layers of bismuth and oxygen. XRD pattern of the sample autoclaved at 373 K (BW-amrph) exhibited a broad peak at ca. 29° and no characteristic peaks, suggesting the absence of crystallites. The absence of a Raman band at 780−850 cm^{-1}, which is assigned to the symmetric stretch mode of WO_6 octahedra[4] and was observed for BW-cryst, also represents the amorphous nature of BW-amrph.

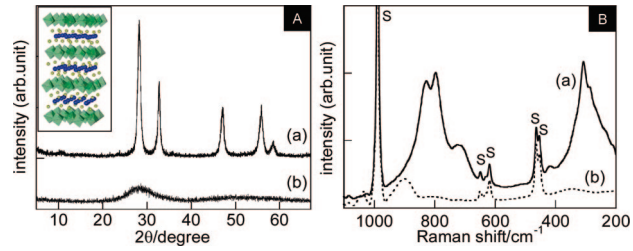

Figure 1. (A) XRD patterns and (B) Raman spectra of (a) BW-cryst and (b) BW-amrph. Symbols "S" in Raman spectra indicate bands assigned to barium sulfate as an internal standard.

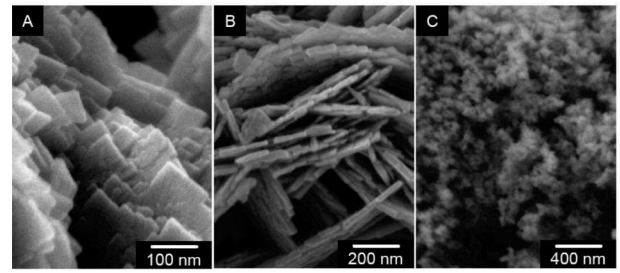

Figure 2. SEM images of (A, B) BW-cryst and (C) BW-amrph.

Figure 2A and B show images of polycrystalline flakes observed in BW-cryst by scanning electron microscopy (SEM). The flakes were composed of stacked rectangular platelets exposing basal (020) planes.[5a] The well-developed morphology of rectangular platelets suggests high crystallinity. The BET specific surface area measured by nitrogen adsorption of BW-cryst was 32 $m^2\ g^{-1}$. The relatively large surface area would have resulted from the small thickness of platelets (20−25 nm) compared to that of previously reported samples autoclaved at 433 K.[6] The BET specific surface area of BW-amrph was 38 $m^2\ g^{-1}$, slightly larger than that of BW-cryst. There was no particle with rectangular morphology in amorphous particles, although we could not obtain a clear SEM image due to the charge up (Figure 2C). Analysis by an energy dispersive X-ray spectrometer equipped with SEM revealed that there were at least no micrometer-sized domains of single metal oxide.

The photocatalytic activity was evaluated by oxidative decomposition of gaseous AcH in air. Decolorization of dyes in an aqueous solution was not employed as a test reaction, because of (1) possible participation of a dye-sensitized process in decolorization, (2) degradation of dyes in a molar amount smaller than that of a photocatalyst, and (3) incomplete decomposition of dye molecules.[7] We have already reported that Bi_2WO_6 crystallites induce complete oxidative decomposition of AcH under UV irradiation.[6b] Here, it was proved that BW-cryst exhibited relatively high photocatalytic activity even under vis irradiation (ca. 8% apparent quantum efficiency at 400 nm) as shown in Figure 3. Complete oxidative decomposition of AcH was proved

[†] Catalysis Research Center.
[‡] Graduate School of Environmental Science.

10.1021/ja807438z CCC: $40.75

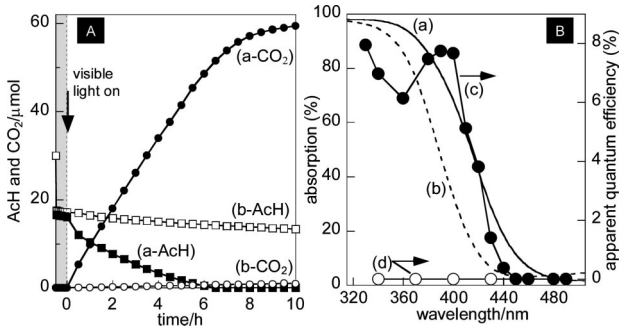

Figure 3. (A) Photocatalytic oxidative decomposition of gaseous AcH (2000 ppm, ca. 30 μmol) over 50 mg of powder of (a) BW-cryst and (b) BW-amrph under vis (>400 nm) irradiation. (B) Diffuse reflectance photoabsorption spectra and action spectra of (a, c) BW-cryst and (b, d) BW-amrph.

by the 2-fold larger yield of CO_2 (60 μmol) than the amount of AcH in the feed. The rates of AcH consumption and CO_2 evolution were much higher than those of Bi_2WO_6 crystallites with a relatively small surface area (data not shown). Preliminary results using Bi_2WO_6 crystallite powders prepared in a similar way suggest that the rates monotonically increased with an increase in their surface area. In this regard, photocatalytic activities of crystal and amorphous Bi_2WO_6 should be compared using samples with similar surface areas. Actually, the photocatalytic activity of BW-amrph was negligible under vis irradiation, although its surface area is sufficiently large to adsorb AcH.

The results of a control experiment of photocatalytic reaction under vis irradiation indicate that the rate of CO_2 liberation over TiO_2 P25 (Nippon Aerosil) was ca. 10 times lower than that over BW-cryst (Supporting Information, Figure S1). The very low activity of P25 proved low contamination of UV in the present irradiation setup. The photocatalyst powder of BW-cryst (50 mg, ca. 72 μmol) could be used repeatedly without deactivation, indicating that the vis-induced reaction was "photocatalytic". The band gap energy estimated from a diffuse reflectance photoabsorption spectrum was ca. 2.8 eV for Bi_2WO_6 crystallites (Figure 3B-a). Since the onset of the action spectrum for BW-cryst was located at 440 nm, the vis-induced CO_2 evolution is assignable to the band gap photoexcitation of Bi_2WO_6 crystallites (Figure 3B-c). It has been suggested that photoexcited electrons in Bi_2WO_6 crystallites promote oxygen reduction without surface modification by platinum or copper oxide required for WO_3.[1]

Negligible photocatalytic activity of BW-amrph not only under vis but also under UV irradiation was confirmed by action spectrum analysis (Figure 3B-b), although BW-amrph absorbs light < 420 nm (Figure 3B-d). It should be noted that the photoabsorption edge was shifted to a longer wavelength by crystallization of the amorphous phase. This result seems reasonable considering that the top of the valence band of russellite is derived from Bi 6s orbitals in addition to O 2p orbitals.[5b]

Figure 4 shows the intensity of transient IR absorption after a 355-nm laser pulse. A clear difference between BW-cryst and -amrph was observed. Rapid buildup of IR absorption was observed only for BW-cryst. Figure S2 shows transient IR absorption spectra. The decay profiles seemed to be independent of the IR wavenumber. The structureless absorption has been reported for photocatalysts such as P25 and assigned to the optical transitions of electrons in the conduction band and/or from shallow midgap states.[8] The electron decay is due to recombination with holes. Appreciable absorbance at 100 μs in BW-cryst indicates slow recombination and a long lifetime of photogenerated carriers to drive appreciable photocatalytic reactions. No transient

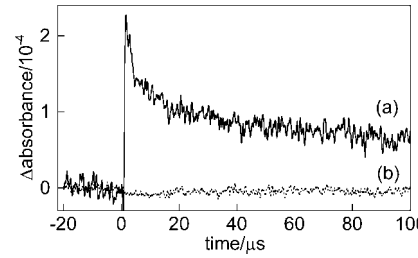

Figure 4. Time profiles of absorbance at 2000 cm^{-1} observed on (a) BW-cryst and (b) BW-amrph irradiated by 355-nm pulse in vacuum.

absorption for BW-amrph indicates fast recombination of electron−hole pairs, resulting in negligible photocatalytic activity.

It should be noted that the conduction band level would be enough for oxygen reduction, since hydrogen liberation over Bi_2WO_6 was reported.[9] However, the decay of the IR absorption was not accelerated by molecular oxygen in this microsecond time scale (data not shown), suggesting reduction of oxygen by photoexcited electrons is not as fast as expected. Further study, at a longer time scale, is needed to understand the mechanism of oxygen reduction over Bi_2WO_6 crystallites.

In summary, Bi_2WO_6 crystallites were found to induce mineralization of AcH under vis irradiation. The photocatalytic activity of amorphous Bi_2WO_6 was negligible due to the fast recombination of charge carriers. It was clearly shown that crystallization to russellite crystallites provided a red shift of the photoabsorption edge and marked increase in the lifetime of photoexcited electrons, resulting in an increase in absorbed photons and photocatalytic reaction efficiency, respectively. The present results indicating a correlation between crystallinity, lifetime of photogenerated carriers, and photocatalytic activity provide essential information for the development of various novel types of metal oxides for photocatalytic environmental purification and solar-energy conversion.

Acknowledgment. We acknowledge useful suggestions by Professor R. Abe (Hokkaido University). This work was supported in part by the Global COE Program (No. B01) from the MEXT, Japan.

Supporting Information Available: Experimental details, result of a control experiment using P25, and transient IR absorption spectra. This material is available free of charge via the Internet at http://pubs.acs.org.

References

(1) (a) Abe, R.; Takami, H.; Murakami, N.; Ohtani, B. *J. Am. Chem. Soc.* **2008**, *130*, 7780–7781. (b) Arai, T.; Yanagida, M.; Konishi, Y.; Iwasaki, Y.; Sugihara, H.; Sayama, K. *J. Phys. Chem. C* **2007**, *111*, 7574–7577. (c) Irie, H.; Miura, S.; Kamiya, K.; Hashimoto, K. *Chem. Phys. Lett.* **2008**, *457*, 202–205.
(2) (a) Ikeda, S.; Sugiyama, N.; Murakami, S.; Kominami, H.; Kera, Y.; Noguchi, H.; Uosaki, K.; Torimoto, T.; Ohtani, B. *Phys. Chem. Chem. Phys.* **2003**, *5*, 778–783. (b) Ohtani, B.; Bowman, R. M.; Colombo, D. P.; Kominami, H.; Noguchi, H.; Uosaki, K. *Chem. Lett.* **1998**, 579–580.
(3) Ohtani, B.; Ogawa, Y.; Nishimoto, S. *J. Phys. Chem. B* **1997**, *101*, 3746–3752.
(4) Graves, P. R.; Hua, G.; Myhra, S.; Thompson, J. G. *J. Solid State Chem.* **1995**, *114*, 112–122.
(5) (a) Zhang, C.; Zhu, Y. F. *Chem. Mater.* **2005**, *17*, 3537–3545. (b) Fu, H. B.; Pan, C. S.; Yao, W. Q.; Zhu, Y. F. *J. Phys. Chem. B* **2005**, *109*, 22432–22439.
(6) (a) Amano, F.; Nogami, K.; Abe, R.; Ohtani, B. *Chem. Lett.* **2007**, *36*, 1314–1315. (b) Amano, F.; Nogami, K.; Abe, R.; Ohtani, B. *J. Phys. Chem. C* **2008**, *112*, 9320–9326.
(7) Ohtani, B. *Chem. Lett.* **2008**, *37*, 217–229.
(8) (a) Yamakata, A.; Ishibashi, T.; Onishi, H. *J. Phys. Chem. B* **2001**, *105*, 7258–7262. (b) Yamakata, A.; Ishibashi, T.; Onishi, H. *J. Mol. Cat. A* **2003**, *199*, 85–94. (c) Yamakata, A.; Ishibashi, T.; Kato, H.; Kudo, A.; Onishi, H. *J. Phys. Chem. B* **2003**, *107*, 14383–14387.
(9) Kudo, A.; Hijii, S. *Chem. Lett.* **1999**, *28*, 1103–1104.

JA807438Z